

Theory of Secondary Emission*

ROBERT G. LYE AND A. J. DEKKER

Electron Physics Laboratory, Department of Electrical Engineering, The University of Minnesota, Minneapolis, Minnesota

(Received May 2, 1957)

The elementary theory of secondary electron emission developed by Salow, Bruining, Baroody, and others has been generalized and modified to incorporate recent measurements by Young of the range-energy relation and the dissipation of energy by slow electrons in solids. It is found that these modifications give considerably improved agreement between the theoretical and experimental "universal" reduced yield curves. However, for primary energies several times higher than that for which the yield has its maximum value, deviations occur; the reduced yield curve for metals appears to lie slightly above the theoretical curve, while that for MgO falls increasingly below. Similar results are found for Ge, but the agreement is better than for MgO.

1. INTRODUCTION

THE emission of secondary electrons resulting from bombardment of a solid with a beam of primary electrons constitutes a complicated theoretical problem. In the first place, an accurate theoretical treatment of the interaction between the primary beam and the lattice electrons requires a detailed knowledge of the band structure of the solid, and of the electronic transition probabilities. Furthermore, the behavior of the excited lattice electrons so produced is complicated by their interaction with other lattice electrons, and by scattering due to phonons and lattice defects. Although there are in the literature several theoretical discussions of a general nature concerning the production¹ of secondary electrons and the escape mechanism,² it is fair to say that it is not yet possible to predict accurately the magnitude of the secondary yield of a given solid for a given initial energy of the primaries. On the other hand, it has been possible to account for fractional changes in the secondary yield of a given solid resulting from variations of a single parameter, such as the temperature³ or the angle of incidence.⁴ Similarly, it has been possible to understand certain trends, such as the relationship between the secondary yield of metals and their work function.⁵ Problems of this nature can be treated, sometimes in a sophisticated manner, because they involve only a single aspect of the complicated mechanism of secondary emission.

In the elementary theory⁶ of secondary emission the

details of the electronic excitation and of the escape mechanism are avoided intentionally since this permits at least a semiquantitative comparison with experiment. One assumes that the secondary yield may be written in the form

$$\delta = \int_0^{\infty} n(x, E_0) f(x) dx, \quad (1)$$

where $n(x, E_0) dx$ represents the number of secondaries produced per incident primary of initial energy E_0 in a layer of thickness dx at a depth x below the surface, and $f(x)$ is the probability that a secondary produced at x arrives at and escapes from the surface. One furthermore assumes that $n(x, E_0)$ is proportional to the energy loss of the primary beam per unit path length, i.e., $n(x, E_0) = -KdE/dx$, evaluated per incident particle (perpendicular incidence will be assumed throughout this paper). Finally, it is assumed that $f(x)$ is given essentially by $\exp(-\alpha x)$, where $1/\alpha$ corresponds to a common effective range of the secondaries in the solid under consideration. It has been assumed in particular that the primary energy losses are governed by Whiddington's law, i.e., $dE/dx = -A/E(x)$, where A is a constant characteristic of the solid. It was first pointed out by Baroody⁵ that on the basis of these assumptions a reduced yield curve could be deduced which was independent of the parameters α , A , and K . That is, if δ_m represents the maximum yield, occurring for a primary electron energy E_{0m} , then a plot of δ/δ_m versus E_0/E_{0m} provides a curve which is independent of the parameters characterizing a particular solid. In fact, Baroody obtained the relation

$$\delta/\delta_m = \frac{1}{F(0.92)} F(0.92E_0/E_{0m}), \quad (2)$$

where

$$F(r) = \exp(-r^2) \int_0^r \exp(y^2) dy. \quad (3)$$

It is striking that experimental data for metals indeed indicate the existence of a universal reduced yield curve. However, the theoretical Baroody curve (2) deviates considerably from the experimental curve for metals,

* Work supported by the Electronic Components Laboratory of the Wright Air Development Center.

¹ D. E. Wooldridge, *Phys. Rev.* **56**, 562 (1939); E. M. Baroody, *Phys. Rev.* **78**, 780 (1950); A. J. Dekker and A. van der Ziel, *Phys. Rev.* **86**, 755 (1952); A. van der Ziel, *Phys. Rev.* **92**, 35 (1953); O. Hachenberg and W. Brauer, *Fortschr. Physik* **1**, 440 (1954); E. J. Sternglass, Report of the Thirteenth Annual Conference on Physical Electronics, Massachusetts Institute of Technology, 1953 (unpublished), p. 55.

² P. A. Wolff, *Phys. Rev.* **95**, 56 (1954); A. J. Dekker, *Physica* **21**, 29 (1954).

³ A. J. Dekker, *Phys. Rev.* **94**, 1179 (1954).

⁴ H. Bruining, *Physica* **3**, 1046 (1936); **5**, 901 (1938).

⁵ E. M. Baroody, *Phys. Rev.* **78**, 780 (1950).

⁶ H. Salow, *Physik. Z.* **41**, 434 (1940); H. Bruining, *Physics and Applications of Secondary Emission* (McGraw-Hill Book Company, Inc., New York, 1954), Chap. 6.

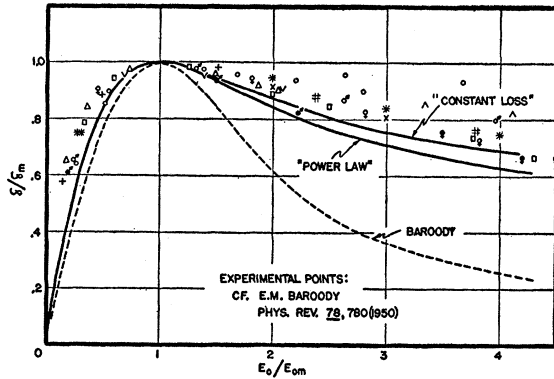


FIG. 1. The curves labeled "constant loss" and "power law" represent respectively formula (17) and (11), both for $n=0.35$. The dashed curve represents Baroody's formula (2). The experimental points, which are included for comparison, are results from the literature which are plotted in Fig. 1 of Baroody.⁵ (The elements which they represent are identified in the caption of that figure.)

particularly in the region beyond the maximum (see Fig. 1). It is the purpose of this paper to show that if one takes into account recent experimental results for the range and energy dissipation of slow electrons in solids, the elementary theory gives good agreement with experiment when the comparison is made on the basis of reduced yield curves. Section 2 gives a generalized power-law theory of secondary emission, i.e., the basic assumptions of the elementary theory are retained but Whiddington's law is replaced by a general power law. In Sec. 3 use has been made of more detailed information concerning the energy dissipation of electrons in solids.

2. GENERALIZED POWER-LAW THEORY

In view of the discrepancy between (2) and the reduced yield curve for metals, one suspects that the Whiddington law may not describe the energy losses of the primaries correctly. In fact, this law gives a penetration depth proportional to the square of the primary energy, whereas Young⁷ concludes from transmission measurements of electrons with energies between 0.3 kev and 7.25 kev through aluminum oxide films that the range-energy relationship for this material is given by

$$R = 0.0115 E_0^{1.35}. \quad (4)$$

Here, the range R is obtained in mg cm^{-2} when the initial primary energy E_0 is expressed in kev. The range as obtained from the experimental data represents the weight per cm^2 by which almost all electrons in the beam have been stopped. It may be noted that the energy dependence of R as expressed by (4) is very nearly the same as that for electrons in the energy range between 0.15 Mev and 0.8 Mev.⁸ Since one does not

⁷ J. R. Young, Phys. Rev. **103**, 292 (1956).

⁸ See for example, Orear, Rosenfeld, and Schluter, *Nuclear Physics* (The University of Chicago Press, Chicago, 1950), revised edition, p. 32.

expect the range-energy relation to vary greatly from one absorber to another, (4) indicates that the Whiddington law probably does not give dependable results for the secondary emission. It thus seems of interest to set up an elementary theory of secondary emission on the basis of an energy loss law for the primaries of the form

$$dE/dx = -A/E^n(x), \quad (5)$$

where for the moment n is an arbitrary power and A characterizes the material.[†]

Integration of (5) yields

$$E^{n+1}(x) = E_0^{n+1} - A(n+1)x, \quad (6)$$

so that the primary range in this case is given by

$$R = E_0^{n+1}/A(n+1). \quad (7)$$

Note that $n=0.35$ produces agreement between (7) and (4). Assuming in expression (1) that $n(x)$ is proportional to $-dE/dx$ and that $f(x)$ is proportional to $\exp(-\alpha x)$, one obtains for the yield

$$\begin{aligned} \delta &= K \left[\frac{A(n+1)}{\alpha} \right]^{1/(n+1)} \exp(-r^{n+1}) \int_0^r \exp(y^{n+1}) dy \\ &= K \left[\frac{A(n+1)}{\alpha} \right]^{1/(n+1)} G_n(r), \end{aligned} \quad (8)$$

where K is a constant which may be considered a measure for the reciprocal of the energy expended by the primary beam to produce an internal secondary and r is given by

$$r^{n+1} = \alpha R = \alpha E_0^{n+1}/A(n+1). \quad (9)$$

Applying the condition $d\delta/dE_0 = 0$ to expression (8), one finds for the maximum of the yield

$$\delta_m = K \left[\frac{A(n+1)}{\alpha} \right]^{1/(n+1)} \frac{1}{(n+1)r_m^n}, \quad (10)$$

where r_m represents the value of r for which the maximum occurs. Hence, from (8) and (10) a universal reduced yield curve is obtained of the form

$$\delta/\delta_m = (n+1)r_m^n G_n(r) = \frac{1}{G_n(r_m)} G_n(r_m E_0/E_{0m}), \quad (11)$$

where $G_n(r)$ is defined by (8). For $n=1$ expression (10) becomes identical with the Baroody expression (2). From what has been said above in connection with expression (4), one may expect n for most substances to be close to the value 0.35. In Fig. 1 expression (11) has been represented for $n=0.35$; it is observed that the agreement with experimental points for metals is

[†] An approximate calculation based on the ad hoc assumption $n=0.5$ has been carried out by A. van der Ziel (private communication).

considerably better than for the Baroody curve (dashed in Fig. 1). The main reason for this is that for primary energies E_0 large compared to E_{0m} expression (11) is proportional to E_0^{-n} , i.e. to $E_0^{-0.35}$ for $n=0.35$; the Baroody function, on the other hand, varies as E_0^{-1} in this energy region. It will be seen later than expression (11) for $n=0.35$ also fits the experimental reduced yield curve for magnesium oxide quite well, for primary energies up to $E_0/E_{0m} \approx 3$.

3. THEORY INCLUDING EFFECTS OF STRAGGLING

Notwithstanding the improved agreement between theory and experiment obtained in the preceding section, objections may be raised against some of the assumptions on which the power law theory is based. These objections are emphasized by the results of recent experiments carried out by Young⁹ on the energy dissipation of low-energy electrons in aluminum oxide. Assuming for the moment that other materials behave similarly, the following conclusions from Young's results may be applied to the theory of secondary emission:

(i) The probability for an electron of given initial energy E_0 to be transmitted through a solid layer of thickness x is approximately given by

$$p(x, E_0) \approx 1 - x/R(E_0), \tag{12}$$

where $R(E_0)$ is the range. Thus, the number of electrons in a beam of given initial energy decreases linearly with the distance below the surface, as represented in Fig. 2.

(ii) When one plots the fraction of energy dissipated by a beam of electrons as a function of the fraction of the range covered, one obtains approximately a straight line through the origin. In other words, the average contribution to $(dE/dx)_{\text{effective}}$ per incident electron is

$$(dE/dx)_{\text{effective}} = -E_0/R(E_0). \tag{13}$$

With reference to conclusion (i), it may be noted that in the power-law theory of the preceding section it was assumed implicitly that the range of all primary electrons is the same. (See Fig. 2.) Thus, expression (12) indicates the importance of straggling of the primaries, which is neglected in the power-law theory. As a con-

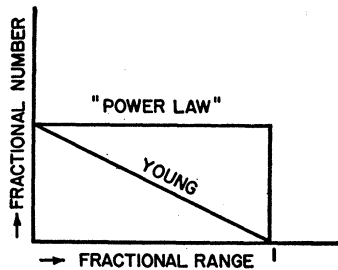


FIG. 2. Idealized representation of the transmission results obtained by Young, reference 9; the curve "power law" indicates the assumption made in the power-law theory.

⁹ J. R. Young J. Appl. Phys. 28, 524 (1957); the authors are greatly indebted to Dr. Young for a prepublication copy of this paper.

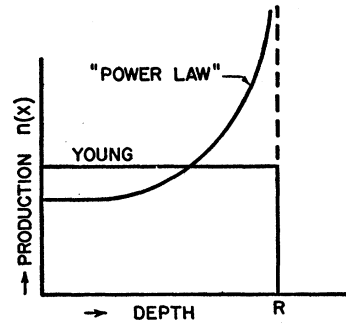


FIG. 3. Idealized representation of the energy dissipation based on Young's measurements, reference 9; the energy dissipation assumed in the power-law theory is indicated for comparison.

sequence of the straggling, the effective energy loss per unit depth evaluated per incident electron will also be different from that calculated on the basis of a single range for all primaries. In fact, if all primaries are assumed to have the same range, most of the energy losses will occur near the end of the range and thus the production of secondaries will be a function of depth as indicated in Fig. 3 by the curve labeled "power law." Straggling, however, would have the tendency of equalizing the energy losses over the range; in fact, according to (13) the losses are essentially constant over the entire range.

It is a simple matter to incorporate this information in the elementary theory of secondary emission. If in (1) one puts $n(x) = KE_0/R$ and $f(x) = \exp(-\alpha x)$, one obtains

$$\delta = (KE_0/\alpha R)[1 - \exp(-\alpha R)]. \tag{14}$$

Writing the range-energy relation in the form $R = CE_0^{n+1}$, where C is a constant, one obtains

$$\delta = KE_0 \frac{1 - \exp(-\alpha CE_0^{n+1})}{\alpha CE_0^{n+1}}. \tag{15}$$

Introducing the function

$$g_n(z) = \frac{1 - \exp(-z^{n+1})}{z^n}, \tag{16}$$

one arrives again at a universal reduced yield curve, viz.

$$\delta/\delta_m = \frac{1}{g_n(z_m)} g_n(z_m E_0/E_{0m}), \tag{17}$$

where z_m represents the value of z for which $g_n(z)$ reaches its maximum value. The function (17) for $n=0.35$ has been represented in Fig. 1, where it may be compared with expressions (2) and (11) (the latter for $n=0.35$), and with experimental points for several metals. It is observed that in the low-energy region (17) and (11) essentially coincide, whereas beyond the maximum (17) lies slightly above (11), thus giving somewhat better agreement with experiment. It may be noted that in the high primary-energy region (17) and (11) both vary as E_0^{-n} .

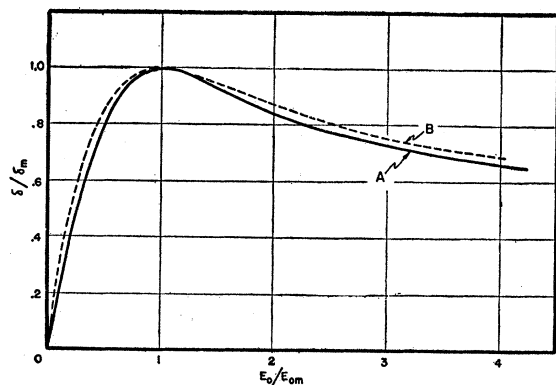


FIG. 4. The solid curve represents expression (19), the dashed curve represents (17), both for $n=0.35$.

A few remarks may be made here in connection with the assumption that the escape mechanism of the secondary electrons can be described by an exponential absorption. In an insulator, secondary electrons with insufficient energy to excite other lattice electrons interact essentially with lattice vibrations only and their behavior can be described in terms of the age theory.¹⁰ Thus, if it is assumed that all secondaries have the same initial energy, the escape probability may be written as

$$f(x) = \text{Erfc}(x/2\tau^{\frac{1}{2}}) \quad (18)$$

where

$$\text{Erfc}y \equiv (2/\pi^{\frac{1}{2}}) \int_y^{\infty} \exp(-z^2) dz.$$

Here, τ is the maximum age of the secondaries, corresponding to the square of the diffusion length over which the energy of the secondaries has been reduced to the electron affinity of the crystal. Combining this escape function with the production term $n(x) = KE_0/R$, based on (13), one can show from (1) that

$$\delta/\delta_m = \frac{1}{L_n(r_m)} L_n(r_m E_0/E_{0m}), \quad (19)$$

where

$$L_n(r) = r \left\{ \text{Erfc}r^{n+1} + \frac{1}{\pi^{\frac{1}{2}} r^{n+1}} [1 - \exp(-r^{2n+2})] \right\} \quad (20)$$

and r_m represents the value for which $L_n(r)$ reaches its maximum value. As shown in Fig. 4, expressions (19) and (17) are very closely the same for $n=0.35$.

4. COMPARISON OF THE THEORY WITH DATA FOR NONMETALLIC SUBSTANCES

In Fig. 5 experimental data have been plotted in the form δ/δ_m versus E_0/E_{0m} for magnesium oxide crystals. The open circles represent data obtained by Whetten and Laponsky¹¹ for a crystal exhibiting a maximum

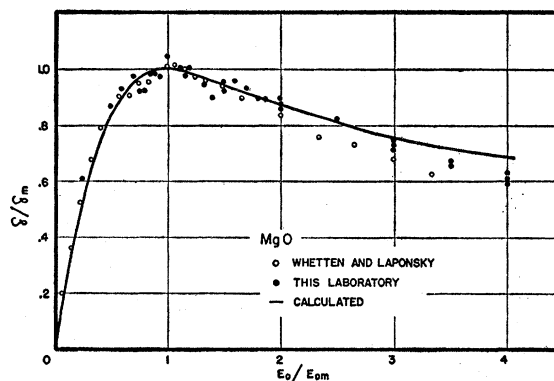


FIG. 5. The solid curve represents equation (17). The experimental points are data for MgO crystals obtained by Whetten and Laponsky (open circles) and in this laboratory (solid circles).

secondary yield of 24 near a primary energy of 1.2 kev. The solid circles refer to measurements made in our own laboratory on a crystal which had been exposed to air; the maximum yield of this crystal was 10.25 near 1.0 kev.

It is observed that in spite of the great difference in yields the data follow rather closely a single reduced yield curve, which implies that, as with metals, the individual crystal characteristics modify the yield curves principally in the role of scale factors and do not influence markedly their functional form. For comparison, the function (17) has been shown in the same figure, calculated on the basis of $n=0.35$. The agreement is good in the region of the yield curve shown, but it should be noted that in contrast to metals, whose reduced yield curve beyond the maximum lies somewhat above the theoretical curves, the yield for MgO lies below, and decreases more rapidly than does the theoretical curve.

At still higher energies, where data for metals are not readily available, we have found that the yield from MgO decreases more nearly as E_0^{-1} , and the function (17) which varies as $E_0^{-0.35}$ deviates rather strongly from the experimental curve.† However, of the functions discussed above which do vary as E_0^{-1} at high energies, viz., (2), and (17) with $n=1$, neither agrees with the experimental data (see Fig. 6). Furthermore, both of these functions presuppose a primary range proportional to the square of the incident energy, which seems improbable in view of Young's results. In Fig. 6 experimental data obtained by Johnson and McKay¹² for germanium are shown also (solid circles), and it is seen that the agreement with (17) for $n=0.35$ is rather better than for MgO although the yield beyond the maximum is again somewhat less than predicted.

¹⁰ M. Hebb, Phys. Rev. **81**, 702 (1951); A. J. Dekker, Physica **21**, 29 (1954).

¹¹ N. R. Whetten and A. B. Laponsky, J. Appl. Phys. **28**, 515 (1957).

† Note added in proof.—Yield curves for Ni and Mo measured to $10 E_{0m}$ by G. Blankenfeld, Ann. Physik **9**, 48 (1951) follow closely the curve for Ge shown in Fig. 6.

¹² J. B. Johnson and K. G. McKay, Phys. Rev. **93**, 669 (1954).

It seems unlikely that the discrepancy at high primary energies can be attributed to a poor approximation to the escape function since in this energy region the yield is determined mainly by the production of secondaries. Better agreement might be obtained for Ge by use of a smaller value for the exponent n , but, as mentioned above, this alone is not adequate for MgO. The origin of the difficulty appears to reside in two approximations used: (a) a mean energy of formation for the secondary electrons which is independent of the primary energy, and (b) a uniform production throughout the range of the primary beam. The first of these would not be expected to hold true over a wide range of energies, and with reference to (b) it should be noted that deviations are expected at high energies on the basis of Young's results.

In conclusion one might say that the modifications of the elementary theory introduced above provide considerably better agreement between the theoretical and experimental reduced yield curves. However, the experimental data show that there does not exist a

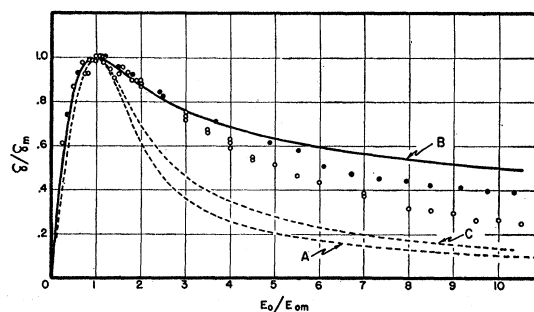


FIG. 6. Curve A represents Eq. (2). Curves B and C represent expression (17) for $n=0.35$ and $n=1.0$, respectively. The open circles are data for the MgO crystal shown by solid circles in Fig. 5, extended to a primary energy of 10.5 kev. The solid circles represent data for a germanium crystal obtained by Johnson and McKay, reference 12.

reduced yield curve which is common to all materials. Variations of the reduced yield curve from one material to another evidently require more detailed considerations of the production and escape mechanisms.

Oscillatory Galvanomagnetic Properties of Bismuth Single Crystals in Longitudinal Magnetic Fields*

JULIUS BABISKIN

United States Naval Research Laboratory, Washington, D. C., and The Catholic University of America, Washington, D. C.

(Received April 18, 1957)

The galvanomagnetic effects of oriented single crystals of bismuth have been studied in longitudinal magnetic fields up to 60 000 gauss at liquid helium temperatures. Oscillatory behaviors with de Haas-van Alphen periodicity were discovered to be superimposed upon the normal galvanomagnetic effects. These results showed that the periods for galvanomagnetic oscillations were independent of the direction and magnitude of the electric current. At high fields, a previously unreported oscillation was observed having a period which compares favorably with the period calculated from parameters for the de Haas-van Alphen effect at the same orientation. At the higher fields and lower temperatures, the galvanomagnetic oscillations exhibited a remarkable resemblance to the exact theory for the oscillatory magnetic susceptibility of a free-electron gas. Both the normal and the oscillatory galvanomagnetic effects are analyzed in terms of a tilted, multi-ellipsoidal model. For one of the orientations studied, the normal longitudinal magnetoresistance exhibited an anomalous maximum, which is attributed to scattering from internal surfaces.

INTRODUCTION AND THEORY

THIS paper has a twofold purpose in that two classes of phenomena, which occur simultaneously in these experiments, are studied. These are: (a) the normal galvanomagnetic effects of oriented single crystals of bismuth in longitudinal magnetic fields (H_L), and (b) the oscillatory galvanomagnetic effects with de Haas-van Alphen periodicity which were observed to be superimposed upon these normal galvanomagnetic effects. These measurements were taken in H_L up to 60 000 gauss and mainly at liquid helium temperatures.

* Based on a dissertation submitted to the Faculty of the Graduate School of The Catholic University of America in partial fulfillment of the requirements for the degree of Doctor of Philosophy.

The normal galvanomagnetic effects of anisotropic single-crystal specimens can be classified¹ into the four following cases:

(a) Longitudinal effects in transverse magnetic fields (H_T) or the transverse magnetoresistance. In this case, $\mathbf{H} \perp \mathbf{J} \parallel \mathbf{E}$ where \mathbf{H} is the applied magnetic field, \mathbf{J} is the electric current, and \mathbf{E} is the measured component of the electric field.

(b) Transverse effects in H_T or the Hall effect ($\mathbf{H} \perp \mathbf{J} \perp \mathbf{E} \perp \mathbf{H}$).

(c) Longitudinal effects in H_L or the longitudinal magnetoresistance ($\mathbf{H} \parallel \mathbf{J} \parallel \mathbf{E}$).

¹ A. H. Wilson, *Theory of Metals* (Cambridge University Press, London, 1953), p. 209.